Boegman, L. 2014. Limitations of hydrodynamic models in simulating Great Lakes processes of varying scale. In proc. Modeling tools for analysis and forecasting of fish recruitment and its response to physical processes. Huron, OH, 23-25 June, 6 pp.

Limitations of hydrodynamic models in simulating Great Lakes processes of varying scale

Leon Boegman, Environmental Fluid Dynamics Laboratory, Department of Civil Engineering, Queen's University, Canada

Introduction: Reynolds-averaged numerical models are routinely applied to simulate waves, currents and turbulence in the Great Lakes. These models have recently been developed to predict transport processes that are relevant to fish recruitment, including egg hatching and larval transport (see work by Zhao, Beletsky, Ludsin, Smith, etc.). The ability of these models for this task depends on the accuracy with which the models reproduce the governing hydrodynamics. The objective of this paper is to describe the abilities, limitations and requirements of Reynolds-averaged models in reproducing physical processes of varying scale in the Great Lakes. Specific processes discussed include basin-scale surface and internal waves, progressive nonlinear internal waves and turbulent mixing.

Basin-scale waves and wave-driven currents: The large-scale circulation and currents in the Great Lakes are primarily forced by basin-scale surface and internal seiches. These low frequency low speed oscillations have wavelengths that scale with the basin size and so are reasonably reproduced on the coarse grids (kms to 100s of m) of Reynolds-averaged lake models (e.g., Boegman et al 2001; Boegman and Rao 2010; Ahmed et al 2013). Unlike smaller lakes, the Earth's rotation affects wave motions in the Great Lakes because the Burger number, $S = Ro/L << 1$, where the Rossby Radius $Ro = c/f$ is the ratio of the wave speed c to the inertial frequency $f = 9.77 \times 10^{-5}$ s^{-1}, at the latitude of the Great Lakes, and $L \sim 100$ km is a characteristic lake lengthscale (typically the lake width). For surface and internal seiches, $Ro \sim (50 \text{ m s}^{-1})/f \sim 500$ km and $Ro \sim (0.5 \text{ m s}^{-1})/f \sim 5$ km, respectively, giving $S > 1$ for surface and $S < 1$ for internal seiches. This means that surface seiches act as planar oscillations along the lake length or width, without significant rotational effects, while slowly propagating internal seiches are affected by rotation.

In the northern hemisphere, the longitudinal seiche becomes a counter-clockwise propagating Kelvin wave, constrained to a lengthscale of $Ro \sim 5$ km from where the thermocline intersects the lakebed (Fig. 1). Similarly, the transverse seiche becomes a clockwise propagating Poincare wave that spans the lake interior. Reynolds-averaged models reproduce Poincare wave motions (Fig. 2), which drive circular particle paths with period, $T = 2\pi/f$ and diameters $D \sim c/f \sim 5$-10 km and significantly influence offshore particle dispersion (Cary Troy, unpublished data). Surface seiches and Poincare waves are, thus, well simulated by lake models (Boegman and Rao 2010; Ahmed et al 2013), but typical the horizontal grid spacing is ~ 500 m < Δx < ~ 5 km and so insufficient to resolve the Kelvin wave with width $Ro \sim 5$ km.

Progressive nonlinear waves and internal surges: Large amplitude internal surges will occur on the thermocline after storm-event forcing (e.g., Boegman and Rao 2010). These surges will steepen until dispersion becomes important and then degenerate into progressive nonlinear internal waves, NLIWs (e.g., Boegman et al 2003; de la Fuente

et al 2010; Boegman and Dorostkar 2011; Vilhena et al 2013). To capture physical dispersion the model horizontal grid spacing must be of the same order as the thermocline depth, which is ~ 10 m (Vitousek and Fringer 2011; Dorostkar 2012). While NLIWs have not been observed in the Great Lakes (nobody has really looked), they have been observed in numerous small (Cayuga Lake (Fig. 3), Seneca Lake, Loch Ness, Babine Lake, etc.) and large (Lake Constance, Lake Biwa, Lake Iseo, etc.) lakes, where they break on the lakebed at the depth of the thermocline causing local mixing and sediment resuspension (Boegman and Ivey 2009).

In addition to the dispersive grid requirement, NLIWs typically have wavelengths of ~100s of m and amplitudes of ~10s of m (Boegman et al 2003; Boegman and Dorostkar 2011). They are, therefore, below the feasible horizontal grid scale of Reynolds-averaged Great Lakes models. Moreover, these waves require nonhydrostatic pressure solvers, which are iterative and take ~10 times longer to converge, compared to the typical hydrostatic solvers. For these reasons, it is not practical to resolve NLIWs in Great Lakes models; for example to simulate 10 days of NLIW propagation in Cayuga Lake (Fig. 3) takes 6 months on 80 CPUs using the MITgcm (Boegman and Dorostkar 2011).

Turbulent Mixing: The smallest scales of motion in the Great Lakes are those associated with turbulent dissipation ε (W kg^{-1}), which is the irreversible loss of fluid momentum to heat by viscous friction, and turbulent mixing K (m^2/s), which is the diffusion of scalar variables by turbulent eddies. Historically, there has been limited research on turbulence in the Great Lakes (Table 1). The rate of ε varies locally with the strength of the currents and stratification and the bed roughness. At typical lake Reynolds numbers, turbulent parameters are anisotropic, with canonical horizontal diffusivities of $K_y \sim K_x \sim 1$ m^2 s^{-1} and vertical diffusivities of $K_z \sim 10^{-3}$ to 10^{-6} m^2 s^{-1} (Table 2).

The smallest motions associated with turbulent eddies occur on scales that are significant for dispersal of fish eggs, larvae and plankton, and likely influence recruitment success (e.g., China and Holzman 2014). These are the Kolmogorov length ($L_\eta \sim 0.3 – 6$ mm), time ($T_\eta \sim 1 – 30$ s), and velocity ($U_\eta \sim 0.2 – 2$ mm s^{-1}) scales (Table 1). Reynolds-averaged models have typical timesteps of minutes and vertical grid spacing of order 500 m – 5 km and 0.5 m - 1 m, respectively, and so sub-grid-scale energy dissipation and diffusion must be parameterized from the resolved mean flow; as must any effects on recruitment. There are many parameterization options, many of which require significant calibration to ensure adequate prediction of observed temperature and current fields. A full description of these parameterizations is beyond the scope of this paper. Some model parameterizations reasonably reproduce turbulent fields (Fig. 4). To directly resolve several days of turbulent motions with Kolmogorov scale grids and timesteps (i.e., a Direct Numerical Simulation) would require a lake volume of ~ 1 m^3 (e.g., Scalo et al 2013). Therefore, lake-wide simulations at these scales are not practical; however, in a very small lake, the largest overturns leading to turbulence have been briefly simulated (Botelho and Imberger 2007).

Conclusions: Using ~500 m horizontal by ~1 m vertical resolution, hydrodynamic models should capture surface and internal (Kelvin and Poincare) seiche motions in the

Great Lakes with runtimes of hours to days. Smaller scale nonhydrostatic features (internal nonlinear waves and hydraulic jumps) would require months of parallel computation on horizontal grids of order 10 m and, therefore, are not feasibly simulated. Grid-averaged turbulent quantities (e.g., dissipation and diffusion) can be correctly parameterized from the resolved mean flow. However, more observations and model-specific validations are required.

References:

Ahmed, S., Troy, C.D., and Hawley, N. 2013. Spatial structure of internal Poincaré waves in Lake Michigan. Env. Fluid Mech. doi: 10.1007/s10652-013-9294-3.

Boegman, L., Loewen, M.R., Hamblin, P.F. and Culver, D.A. 2001. Application of a two-dimensional hydrodynamic reservoir model to Lake Erie. *Can. J. Fish. Aquat. Sci.* 58: 858-869.

Boegman, L., Imberger, J, Ivey, G.N. and Antenucci, J.P. 2003. High-frequency internal waves in large stratified lakes. *Limnol. Oceanogr.* 48: 895-919.

Boegman, L. and Yerubandi, R. Rao. 2010. Process oriented modeling of Lake Ontario hydrodynamics. Proceedings *6th International Symposium on Environmental Hydraulics*, Jun. 23-25, Athens, Greece, 6 pp.

Boegman, L., and Dorostkar, A. 2011. Three-dimensional simulation of NLIW generation, propagation and breaking in Cayuga Lake. Proceedings *7th Int. Symp. on Stratified Flows*, Rome, Italy, August 22 - 26, 2011, 8 pp.

Boegman, L., and Ivey, G.N. 2009. Flow separation and resuspension beneath shoaling nonlinear internal waves. *J. Geophys. Res.* 114, C02018, doi:10.1029/2007JC004411

Botelho, D. and Imberger, J., 2007, Down-Scaling Model Resolution to Illuminate the Internal Wave Field in a Small Stratified Lake, Journal of Hydraulic Engineering (ASCE), 133:1206-1218

China, V. and Holzmana, R. 2014. Hydrodynamic starvation in first-feeding larval fishes. PNAS doi/10.1073/pnas.1323205111

de la Fuente, A., K. Shimizu, Y. Niño, and J. Imberger. 2010, Nonlinear and weakly nonhydrostatic inviscid evolution of internal gravitational basin-scale waves in a large, deep lake: Lake Constance, J. Geophys. Res., 115, C12045, doi:10.1029/2009JC005839.

Dorostkar 2012. Three-Dimensional Dynamics of Nonlinear Internal Waves. PhD Thesis, Department of civil Engineering, Queen's University.

Vilhena, L.C., Clelia L. Marti and Jörg Imberger, The importance of nonlinear internal waves in a deep subalpine lake: Lake Iseo, Italy. Limnol. Oceanogr., 58(5), 2013, 1871-1891 | DOI: 10.4319/lo.2013.58.5.1871

Vitousek, S. and O. Fringer. 2011. Physical vs. numerical dispersion in nonhydrostatic ocean modeling. *Ocean Modelling*, 40(1):72 – 86

Table 1: Typical Kolmogorov length L_η, time T_η, and velocity U_η scales from observations in Lake Ontario and Lake Erie. The kinematic viscosity $\nu \approx 10^{-6}$ m^2 s^{-1}.

Location	**ε (W kg^{-1})**	**$L_\eta = (\nu^3/\varepsilon)^{1/4}$ (mm)**	**$T_\eta = (\nu/\varepsilon)^{1/2}$ (s)**	**$U_\eta = (\nu\varepsilon)^{1/4}$ (mm s^{-1})**	**Source**
Central Lake Erie nearshore	10^{-7}	1.8	3.2	0.56	Bouffard et al 2013
Central Lake Erie offshore	10^{-9}	5.6	31	0.18	Bouffard et al 2013
Western Lake Ontario surface layer	10^{-4} to 10^{-5}	0.32 to 0.56	0.10 to 0.31	1.8 to 3.2	Terray et al 1996
Lake Ontario nearshore hypolimnion	10^{-8}	3.2	10	0.32	Paturi et al 2013
Lake Ontario nearshore surface layer	10^{-5}	0.55	0.30	1.8	Palmer 1973
Lake Ontario offshore surface layer	10^{-4}	0.32	0.11	3.1	Palmer 1973

Table 2: Typical vertical (diapycnal) diffusivities from observations in Lake Ontario and Lake Erie.

Location	**K_z (m^2 s^{-1})**	**Source**
Western Lake Erie nearshore	6×10^{-4} to 5.5×10^{-3}	Edwards et al. 2005
Western Lake Erie offshore reef	1.7×10^{-3} to 4.1×10^{-3}	Ackerman et al. 2001
Central Lake Erie watercolumn	6.5×10^{-6}	Bouffard and Boegman 2013
Western Lake Ontario nearshore	10^{-3}	Rao and Murthy 2001
Central Lake Erie watercolum	10^{-4} to 10^{-5}	Rao et al. 2008

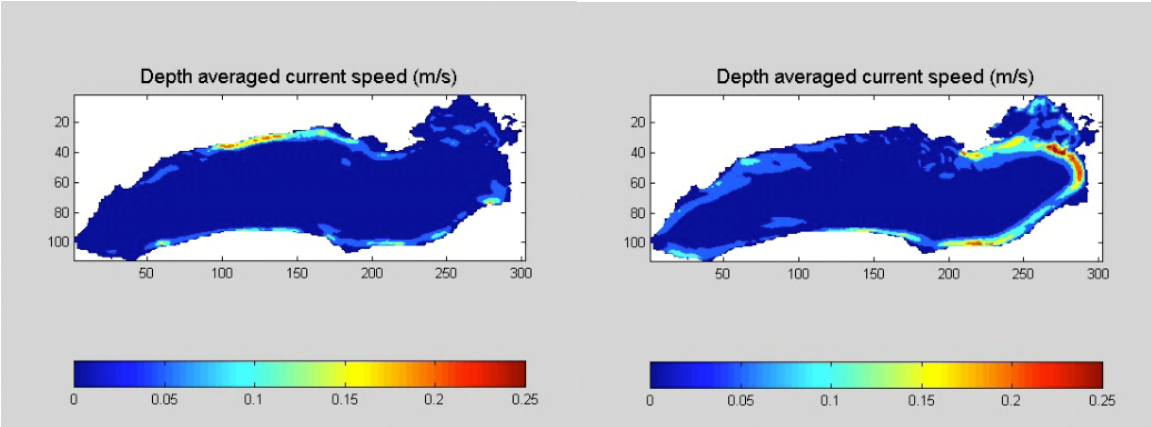

Figure 1: Depth-averaged current speed from ELCOM showing two phases of the Kelvin wave propagation around Lake Ontario after an idealized wind forcing event. Unpublished figure from simulations described in Boegman and Rao (2010).

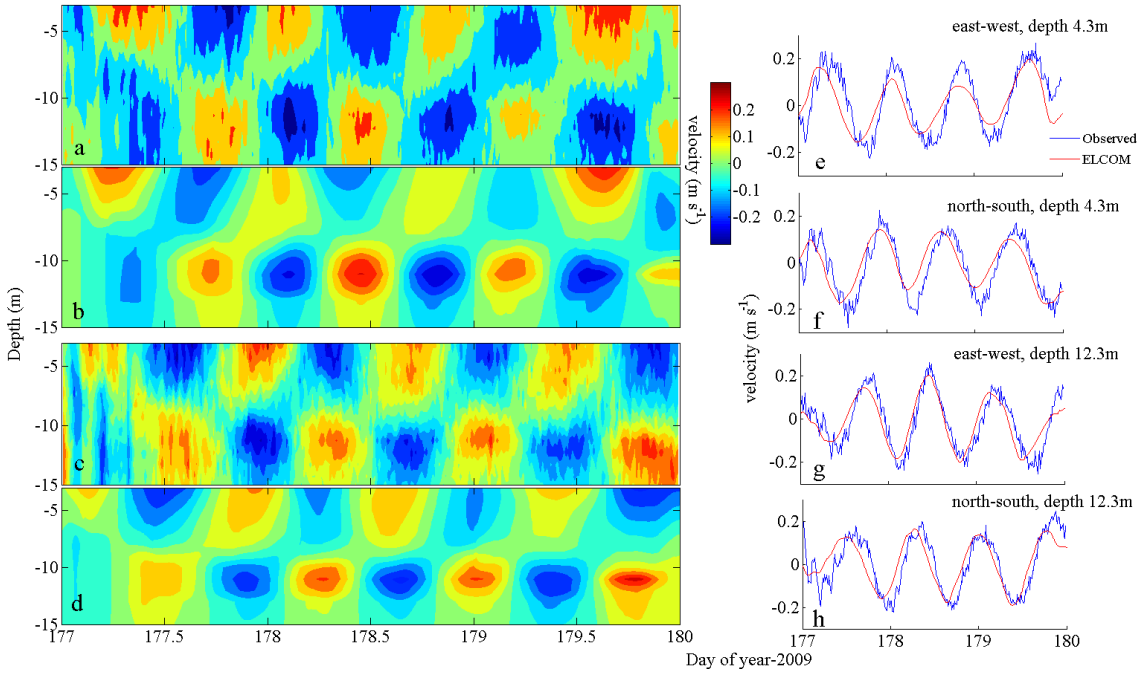

Figure 2: Observed and ELCOM modeled Poincare wave-induced velocity field Sta. 341 in central Lake Erie during 2009. (a) Observed and (b) modeled east-west velocity component; (c) observed and (d) modeled north-south velocity component. (e)-(h)Time series of observed and modeled velocity at 4.3 m and 12.3 m depths in east-west and north-south directions, as indicated. From Valipour, Bouffard, Boegman and Rao, submitted to Limnol. Oceanogr.

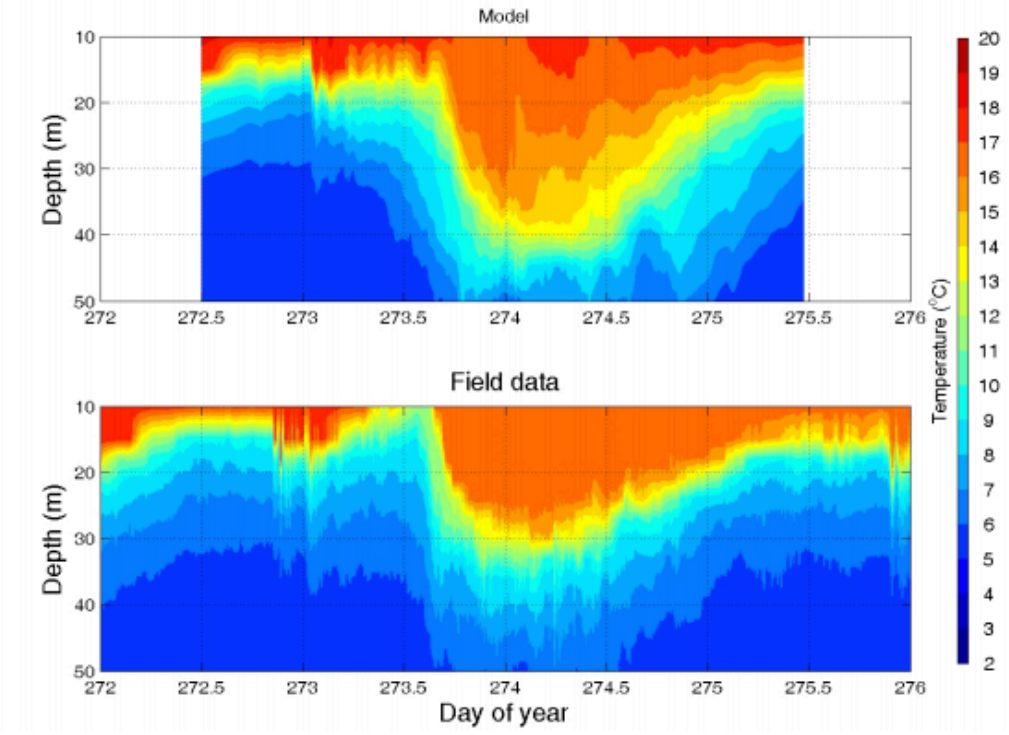

Figure 3: (a) Observed and (b) MITgcm modeled NLIW packet (day 273) and internal surge (day 274) in Cayuga Lake during 2006. From Boegman and Dorostkar (2011).

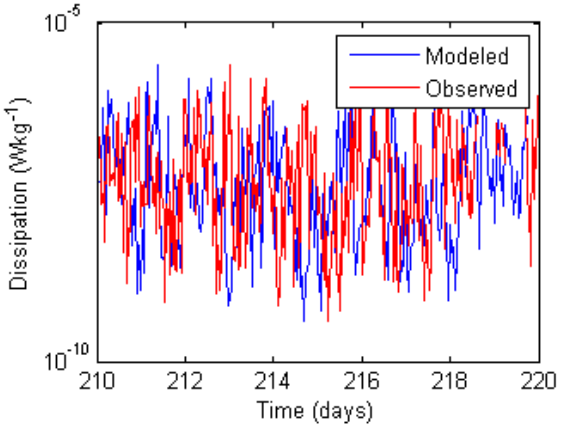

Figure 4: Observed and modeled (using the ELCOM model) turbulent dissipation 1 m above the bed on the 20 m isobaths offshore from Port Hope, Ontario. From Paturi, Boegman, Bouffard and Rao, submitted to J. Hydraulic Eng.